Available online at www.sciencedirect.com
SCIENCE DIRECT®
Journal of Hydrology 302 (2005) 1–12
Journal of Hydrology
www.elsevier.com/locate/jhydrol

Influence of hydrological and climatic parameters on spatial-temporal variability of fluorescence intensity and DOC of karst percolation waters in the Santana Cave System, Southeastern Brazil

F.W. Cruz Jr.[a], I. Karmann[a,*], G.B. Magdaleno[b], N. Coichev[b], O. Viana Jr.[a]

[a]*Instituto de Geociências, Universidade de São Paulo, Rua do Lago, 562, CEP 05508-080 São Paulo-SP, Brazil*
[b]*Instituto de Química,Universidade de São Paulo, CP 26077, CEP 05513-970 São Paulo-SP, Brazil*

Received 24 April 2003; revised 7 June 2004; accepted 10 June 2004

Abstract

Fluorescence intensity (FI) and organic carbon concentration of groundwater percolating through soil and rock into the Santana Cave were monitored at eight different cave sites between 2000 and 2002 to investigate their relationships to climatic parameters, stalactite discharge and thickness of rock overlying the cave. FI values, compared among sampling sites, are inversely proportional to depth and directly proportional to discharge; in contrast, dissolved organic matter (DOC) shows no significant spatial variability. Time-series analysis demonstrated similarities in DOC trends of different waters, but no correlation was observed with FI trends. Combined evaluation of DOC of infiltration waters, rainfall data and chemical parameters of Fe, O_2, pH, Eh in soil solution indicate that peaks in DOC content coincide with more reduced conditions in the soil and have a lag time of 2–3 months after heavy showers. Variation of FI throughout the year occurs at all sampling sites but only higher drip discharge and rimstone pool waters were correlatable to rainfall events. FI of lower discharge sampling sites shows similar trends, but no relationship between drip discharge and rainfall variation was observed. Ranges and means of FI for all drip waters were significantly higher in the 2001–2002 period than in the preceding 2000–2001 period, which correlates with a 5.5 °C increase in mean austral winter temperatures in 2001. Hence, FI variations of karst waters that form carbonate speleothems under a humid subtropical climate may provide a useful proxy in paleoenvironmental reconstruction.

Keywords: Fluorescence; Karst; Groundwater; DOC; Hydrology; Climate

1. Introduction

The UV fluorescence of organic matter extracted from soil and dissolved in marine and fluvial waters has been intensely studied as a potential natural tracer

* Corresponding author. Fax: +55-11-3091-4138.
E-mail address: ikarmann@usp.br (I. Karmann).

0022-1694/$ - see front matter © 2004 Elsevier B.V. All rights reserved.
doi:10.1016/j.jhydrol.2004.06.012

since it is possible to identify different sources of waters based on their fluorescence intensity (FI) and wavelength (WL) (Coble et al., 1990; Senesi et al., 1991; De Souza Sierra et al., 1994; Coble, 1996). However, few authors have applied these parameters to groundwater studies.

Baker and Genty (1999) attributed variations of FI and WL of drip waters in caves and mines from different areas to differences mainly in the vegetation cover, soil type and soil wetness, although the causes of such variations are not yet well understood. Based on the relationship between excitation and emission wavelength, these authors suggested that organic compounds with higher WL are probably absent and that fulvic acids and proteins are the main fluorophores in groundwater.

Previous studies of fissured and karst aquifers in regions of temperate climate demonstrated that variations in FI are related to events of rainwater recharge, which are responsible for erosion or lixiviation of soil organic matter (SOM) and their transport to the drip waters in the cave (Baker et al., 1997; Baker and Barnes, 1998). A direct relation between FI variations and the dissolved organic carbon (DOC) of karst percolation waters was suggested. In this case, the increase of DOC values is due to enhancement of the capacity of transport of organic matter which occurs in response to recharge increase of the system during rainy periods. In addition, the mobility of subcomponents of SOM is likewise enhanced by the increase in the proportion of smaller, more hydrophilic components rather than larger and more hydrophobic components in solution (McCarthy et al., 1993; Kalbitz et al., 2000; Kalbitz, 2001). Both composition and transport of DOC from the soil to drips feeding speleothems are influenced by climatic conditions (McGarry and Baker, 2000).

Recent research on FI and WL in carbonate deposits has shown that it is possible to get high resolution paleoclimate records from carbonate speleothems which allow interpretations of changes in vegetation (Baker et al., 1996) and paleoprecipitation (Baker et al., 1993, 1999b; Charman et al., 2001). However, the interpretation of FI variations in speleothems should be calibrated by the present day relationship between fluorescence properties of the water and climatic parameters in the area of the cave (Baker et al., 1999a).

In order to support future reconstruction of paleoclimate based on fluorescence variations of ancient speleothems of Southeastern Brazil, this study presents relationships between present day climatic parameters and temporal and spatial variations of FI and DOC of percolation waters from a karst system where soils and speleothems are developing under humid subtropical climate and dense vegetation. In addition, the influence of hydrogeological characteristics, such as rock overburden thickness and drip discharge on the FI and DOC values of percolation waters is considered in the discussion of the effect of groundwater residence time in the vadose zone and the filtering effect of the fissure network in the rock on the organic substances in solution.

2. Study area and sampling sites

The Santana Cave is located in Iporanga municipality, 350 km South of São Paulo City, Southeastern Brazil, approximately 100 km from the Atlantic coast (Fig. 1a). The cave, with 6.3 km of conduits, is developed in low-grade metamorphic limestones of the Meso- to Neoproterozoic Açungui Group (Campanha and Sadowski, 1999). The topography of the karst system exhibits large differences in altitude and, consequently, significant variations in the thickness of the vadose zone above the cave (Fig. 1b). The area of the cave is densely vegetated with Atlantic rainforest. Analyses of FI and DOC were performed on waters from runoff, soil and eight sampling sites in the cave. Sampling took into account different hydrological conditions represented by aquifer thickness between 100 and 300 m and mean drip water discharge between 55 and 3.5×10^5 ml/h (Table 1). Soil water was sampled from a well at a depth of 4–5 m in clayey soils above the epikarstic zone (Fig. 1b). Runoff was sampled nearby in a small temporary stream during rain events. Both runoff and soil water samples were unsaturated with respect to $CaCO_3$, with a saturation index of -2.4 and -1.9, respectively (Viana Jr., 2002).

Four cave sites (ESF, EIF, TSF, TIF) are closely distributed around the Salão das Flores, a fossil tributary of the cave river (Fig. 1b). This point is located 100 m below the surface, 35 m above the river level at the main gallery and 150 m from the cave

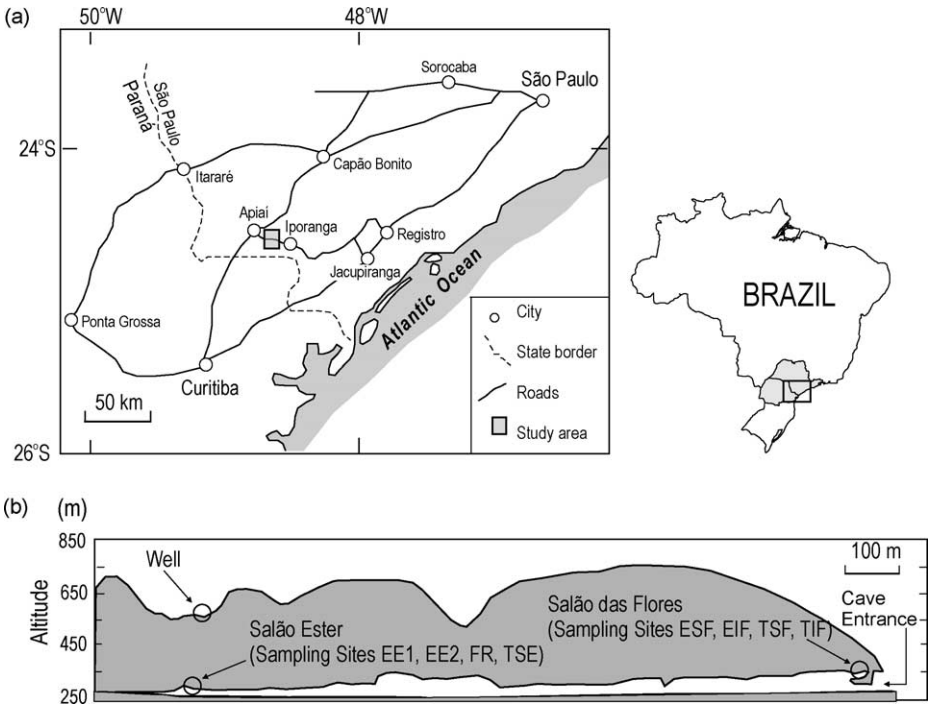

Fig. 1. (a) Location map of study area. (b) Cave longitudinal profile showing the location of the sampling sites with depth and distance from cave entrance.

entrance. The other four sites (EE1, EE2, TSE, FR) are located in the Salão Ester, 300 m below the surface and about 1,500 m from the cave entrance.

In both locations, with exception of EIF, the sampling sites were active throughout the year. ESF, EEI, EE2 and EIF are stalactite drip waters characterized by lower discharge when compared to FR, which is a small waterfall in the cave (Table 1). TSF, TSE and TIF are accumulations of water in small rimstone pools on the cave floor fed by water from the ESF, EE2 and EIF stalactites, respectively.

Table 1
Results from fluorescence intensity, drip discharge and dissolved organic matter for runoff, soil and cave waters

Sampling site	Fluorescence intensity (FI)						Discharge (ml/h)	CV (%)	DOC (mg/l)	CV (%)
	Mean	*n*	Min	Max	Range	CV (%)				
Runoff	7391	5	4001	9999	5998	34				
Soil	2083	9	815	3596	2781	39			8.2	85
TSF	851	9	489	2257	1768	64			10.23	51
TIF	629	7	526	989	463	26			7.2	49
TSE	402	9	186	886	700	51			8.83	77
EIF	2758	18	520	9990	9470	101	818	>200	5.0	116
FR	1167	22	239	6530	6291	114	3.50×10^5	9.0	10.49	60
ESF	1576	22	378	5119	4741	83	120.99	12.7	8.84	63
EE1	1699	22	188	5740	5562	93	470.51	15.2	6.61	81
EE2	856	23	196	2749	2553	65	55.09	8.1	8.34	80

CV = coefficient of variation.

3. Sampling and analytical methods

Water sampling for FI at drip water sites (ESF, EE1, EE2, EIF) was performed between September 2000 and June 2002. The sampling frequency at these sites varied between 1 month to 15 days. The EIF site was not active between September and December 2000. Sampling in rimstone pools and soil waters was carried out between September 2000 and June 2001. Sampling for DOC was performed from September 2000 to March 2002 at ESF and EE2 sites. Because of logistical problems, the DOC sampling period at the other sites was shorter.

Surface and cave water samples for fluorescence and DOC analysis were collected in 15 ml amber glass bottles. The samples for ion analysis were collected in 50 ml high density Nalgene polyethylene bottles. Bottles were previously cleaned with non-fluorescent detergent, dilute perchloric acid and rinsed with deionized water. Soil water samples were pumped out of the well using a Low Flow Waterra inertial pump with high density polyethylene tubes (previously cleaned with dilute HCl) from which the water samples were rapidly transferred to the bottles.

For DOC and ion analysis, samples were preserved by adding 12 drops of 10% phosphoric acid and 2–3 drops of concentrated nitric acid, respectively. These samples were kept refrigerated at 4 °C until analysis. Samples for fluorescence analysis were frozen for 5–10 days. All samples were filtered through Millipore HA2500 filters (pore size 0.45 μm) prior to analysis.

pH, Eh and dissolved oxygen were measured immediately after each collection using an Orion Multi-Parameter Model 1230 with the following probes: Orion Model 9107 WP, Orion Model 9778 BN, and Orion Model 083010, respectively.

Precipitation and stalactite discharge were measured automatically using a Davis automatic tipping bucket gauge coupled to an Onset Logger, model Hobo for 8000 events. The discharge values were continuously recorded on the loggers at the slowest drip water flows (EE2 and ESF), over an interval of 17–21 days for ESF and 8–12 days for EE2, depending on the flow changes during the year. At other cave sites, discharge measurements were based on the time elapsed to fill a container of known volume.

Temperature and relative humidity (RH) were measured automatically, every 30 min, using an Onset Hobo RH-Temp logger H8-series at Salão Ester and Salão das Flores in the cave and at the surface in the forest near the water-sample collection sites. Monthly variance of RH values was calculated as follows: $\mathrm{Var} = n\Sigma x^2 - (\Sigma x)^2/n^2$, where n is the number of observations and x is the mean daily value. Because of technical problems with the RH sensor, variance values were not obtained for the period between May 2001 and September 2001.

DOC samples were analyzed using a Shimadzu TOC-5000 analyzer. The results are expressed as the mean of triplicate analyses with analytical errors of approximately 1%. Ion analyses of water samples were made by inductively coupled plasma optical emission spectroscopy (ICP-OES) using an ARL 3410 instrument with a CETAC ultrasonic nebulizer model U 500 AT (precision of $\pm 1\%$).

The FI of water samples was determined using a Hitashi F-4500 luminescence spectrophotometer. The excitation source was a xenon lamp. The slits were set at 10/20 nm for excitation and emission. The photo-multiplier was operated at 950 V. The samples were placed in 2.0 ml quartz cells with a 1.0 cm optical path length.

Fluorescence analyses with excitation at 300 nm and emission wavelength at 430 nm were carried out for water samples at 25 °C. Stability of the machine was tested based on the Raman peak of deionized water excited at 350 nm, after every 5–20 analyses.

Differences in DOC and FI between sites were tested using the one-way ANOVA procedure in order to examine the effects of discharge and depth on their variability.

4. Results and discussion

4.1. Climate in the studied area

The climate of the region is subtropical humid, with rainfall and relative humidity uniformly distributed throughout the year (Nimer, 1989). The mean annual precipitation at the Bairro da Serra Station, located 7 km from the Santana Cave entrance, was 1631 mm from 1973 to 2000 (source DAEE: www.daee.sp.gov.br). During this period, the maximum and minimum values for annual precipitation were 1860 and 1069 mm, respectively. Although the rainfall is

uniformly distributed throughout the year, winter (June–August) is usually drier than summer (December–March). Monthly mean precipitation, temperature and variance of relative humidity monitored from August 2000 to June 2002 over the Santana cave are presented in Fig. 2. Precipitation was highest from November 2000 to January 2001 and in October 2001.

Temperature between July 2000 and June 2002 ranged from −0.2 to 28.3 °C, averaging 18.6 °C. Like the precipitation values, mean monthly temperature varied significantly during the studied period (Fig. 2b), with the lowest temperatures recorded in June/July (winter) and the highest in February/March (summer). The range between winter and summer in 2000–2001 and 2001–2002, were 12.9 and 7.4 °C, respectively, as a consequence of an increase of 5.5 °C in mean winter temperature in 2001.

Although the mean relative humidity (RH) in the atmosphere under influence of a dense rain forest is close to 100% during the year, there are diurnal fluctuations directly related to insolation. RH decreased to as little as 60% during the day, returning to saturated conditions in the late afternoon. Variance of mean monthly humidity, based on mean daily values, was highest between October and December of 2001, indicating less humid conditions for this period (Fig. 2b). During the other months, RH variance changed slightly, with lowest humidity in February and March (lowest values of RH variance).

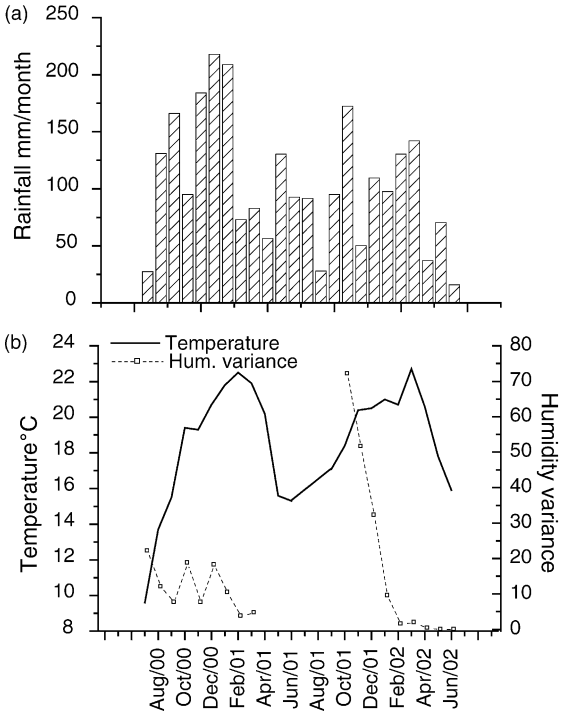

Fig. 2. Climatic parameters in the Santana Cave area. (a) Monthly rainfall variations. (b) Temperature and variance of relative humidity.

4.2. FI and DOC concentration of the waters

The FI and DOC results for runoff, soil and cave waters are presented in Fig. 3 and Table 1. Comparing the different waters, it can be seen that values for FI decrease significantly along the infiltration pathway from surface to drip waters.

The highest FI values, observed in all waters between September/2000 and March/2001, are in runoff waters (7391 ± 2265, $n=5$), followed by soil water at a depth of 4–5 m deep (2083 ± 818, $n=9$), cave drip waters (1699 ± 1587, $n=107$), and rimstone pool waters (627 ± 395, $n=25$).

Although FI values for soil and cave waters show significant variations, the DOC of the samples did not vary with depth along the infiltration pathway. DOC concentrations of the samples range from 1 to 25 ppm and do not define fields in the graph of FI vs. DOC (Fig. 3). In the same plot, there is no obvious correlation between FI and DOC. These results suggest that FI values cannot be directly related to

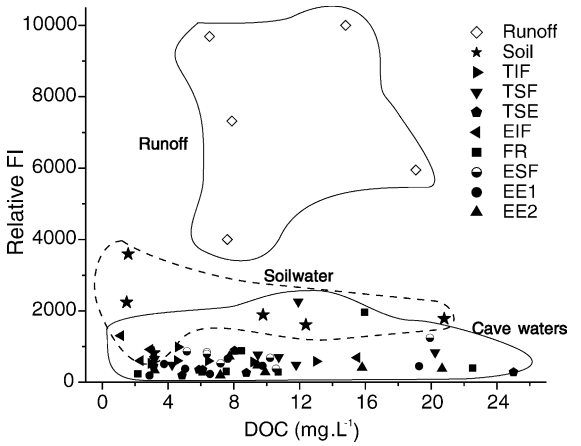

Fig. 3. Scatterplot of fluorescence intensity and dissolved organic carbon variations for runoff, soil and cave waters between September/2000 and March/2001.

total DOC, but more probably reflect the differing proportions of fluorophores.

4.3. Temporal variation of DOC

DOC results for soil water, rimstone pools and cave drip waters from EIF and FR are presented in Fig. 4b. In order to investigate possible causes of the variations in soil water DOC, other parameters, such as Fe and dissolved oxygen concentrations, pH and Eh for soil waters, were compared with the DOC curve in Fig. 4c–f.

All sampled cave waters collected prior to March 2001 show small variations of DOC for most of the time (mean of 7.22 ± 2.07, $n = 32$). However, samples collected in March 2001, presented an anomalous increase in DOC values at all sites (mean of 21.52 ± 2.07, $n = 5$), 64% above the mean concentration for the preceding period (Fig. 4b, Table 1).

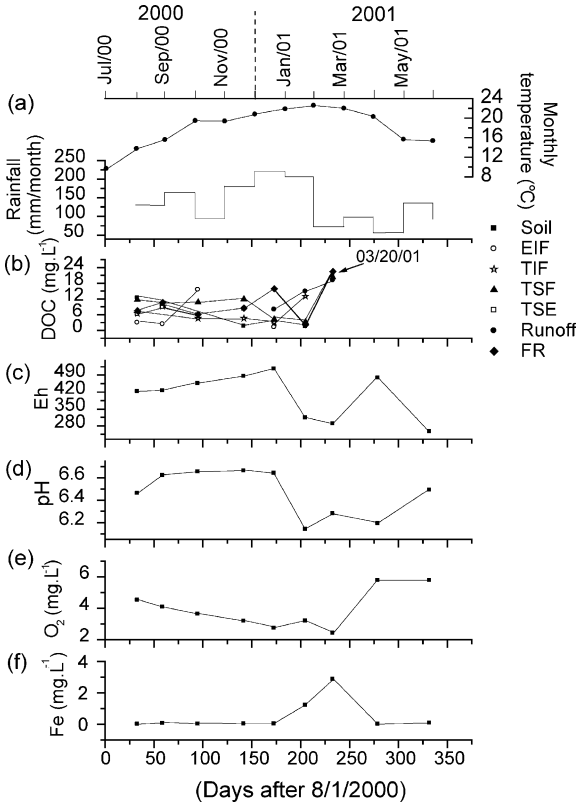

Fig. 4. Compared variations of: (a) monthly rainfall and mean temperature variations; (b) DOC in soil, rimstone pools and rapid flow sites and chemical parameters in soil water; (c) Eh; (d) pH; (e) dissolved O_2; and (f) Fe concentration.

Simultaneously with the increase in DOC content of all waters (Fig. 4b), Fe concentration rose to detectable values while pH, Eh and dissolved oxygen of the soil water decreased (Fig. 4c–f). The combination of these parameters indicate that more reduced conditions were dominant in March 2001 and Fe^{+2} was present in solution, according to the relationship between pH and Eh as expressed by the Nernst equation (Krauskopf, 1979). The high DOC values of March 2001 (Fig. 4b) occurred under more reducing conditions in the soil and are coincident with the reduction in rainfall (Fig. 4a). There is a lag of 2 months between the rainfall maximum and the peak in DOC. During the period of high precipitation and temperature, December 2000–January 2001 (Fig. 4a), increased biological activity enhanced organic matter production. This biological activity was favored by increased water content in the soil due to diffusion and greater availability of oxygen provided by this water (Linn and Doran, 1984; Balesdent et al., 2000). In addition, biological activity may also be intensified by temperature and RH increases (MacDonald et al., 1995; Zogg et al., 1997). The lag between precipitation maximum and DOC peaks may be explained if organic matter produced earlier only went into solution two months later when soil conditions began to become less humid.

High microbial activity favors the mineralization of SOM within pores of fine sediments in soils, protecting it against erosion or leaching (Sollins et al., 1996). On the other hand, the microbial population decreases with reduced soil water reduction (as observed in March 2001), which for instance could be responsible for the destabilization of SOM with consequent increase of DOC (Golchin et al., 1994; Puget et al., 1995; Balesdent et al., 2000).

The sampling for DOC in the slow drip waters was extended for a longer period (September 2000–February 2002) at ESF (at a depth of 100 m) and EE2 (at a depth of 300 m), where stalactite discharges were monitored automatically (Fig. 5). Samples for DOC at EE1 site (at a depth of 300 m) were collected from September 2000 to November 2001.

DOC variations in slow drip waters show trends similar to those at the other sampling sites until March 2001 (Figs. 4b and 5b). This result suggests that DOC

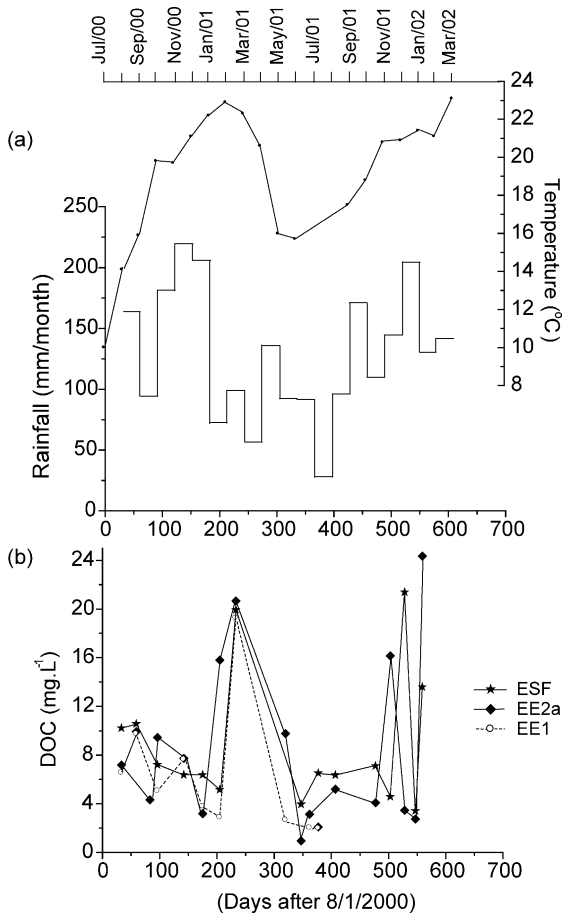

Fig. 5. (a) Monthly rainfall and mean temperature variations. (b) Time series of dissolved organic carbon variations for slow drip waters sites at 300 m deep (EE1 and EE2 sites) and at 100 m deep (ESF).

differences with depth along the infiltration pathway of meteoric water in a deep karst system are not significant, in contrast to the relationship observed in topsoils (Kalbitz, 2001) and a 1.5–3 m deep sand aquifer (McCarthy et al., 1993).

In addition to the DOC peak of March/2001, other peaks observed between December 2001 and February 2002 at the ESF and EE2 sites (Fig. 5b) also exhibit time lags of 2–3 months relative to heavy rains (Fig. 5a). They represent an increase of more than 200% in comparison to the mean values of DOC for both ESF and EE2 drip waters. The correlation between the DOC variations at ESF and EE2 sites is statistically significant by the Anova Test ($p=0.81$, $\alpha=0.05$, $n=15$).

Considering that discharges of cave drip waters exhibit differences of more than two orders of magnitude, a significant dilution of SOM would be expected, leading to lower DOC in drip waters with higher discharge. However, this dilution has not been observed and thus may be explained by the homogenization of dissolved SOM in waters at the beginning of their infiltration in soil.

4.4. Temporal and spatial variation of FI

FI results of karst percolation waters are presented in two groups based on distinct flow characteristics and similarities in the FI signal through time. Group I is represented by soil, rimstone pools (TSF, TSE, TIF) and fast drip stalactites (FR and EIF) and group II by slow drip stalactites (ESF, EE1 and EE2).

4.4.1. Soil, rimstone pools and fast drip stalactites

The monthly FI variation of the first group (TSF, TSE, TIF, FR and EIF) is presented in Fig. 6 and summarized in Table 1. The mean FI values of these waters confirm the decrease in FI with increasing depth. The highest mean FI values are observed in runoff water (7391 ± 2532, $n=5$), followed by soil water (2083 ± 818, $n=9$), fast dripping waters at EIF site (2758 ± 2782) and at FR site (1167 ± 1331), rimstone pools located 100 m beneath the surface, TSF (675 ± 133, $n=8$) and TIF (568 ± 33, $n=6$), and rimstone pools located 300 m beneath the surface, TSE (342 ± 102, $n=8$). The inverse relationship between FI and depth is apparently a consequence of preferential retention and fractionation of SOM components (Fluorophores) due to filtration within the rock fissure network, as no systematic differences in DOC values are observed (Fig. 4b).

FI variations of the group I samples from September 2000 to June 2001 exhibit a peak in December, correlated with maximum local rainfall (Fig. 6). During this period an abrupt increase of 234, 174 and 259% relative to mean values of FI was observed respectively, in waters at TSF, TIF and TSE sites. The peaks of FI observed at these sites did not coincide with the anomalous values of DOC in March 2001 (Figs. 4b and 6b). This indicates that FI variations are related more to selectivity and availability of certain SOM components in the system

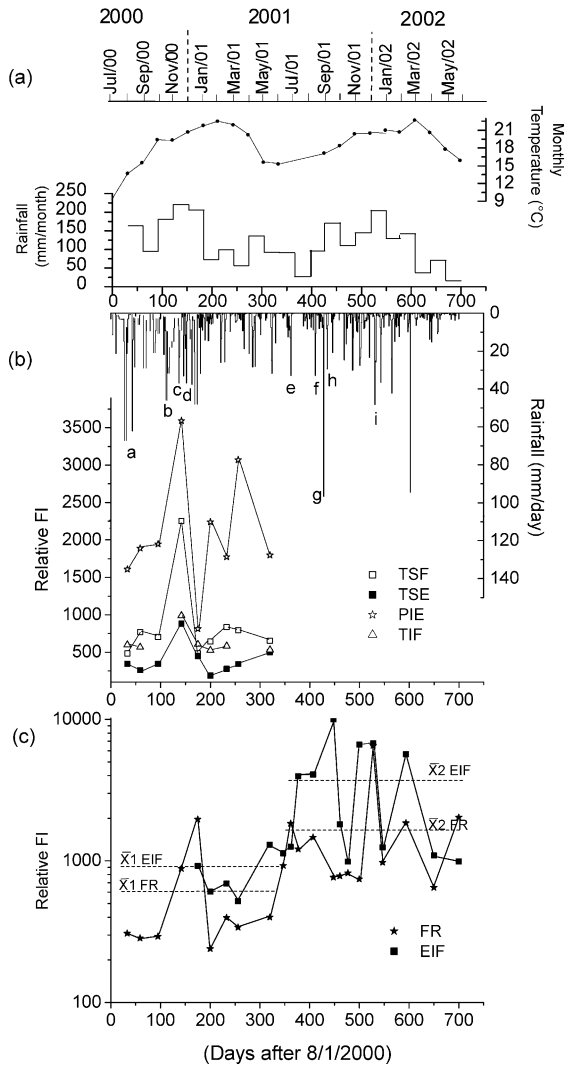

Fig. 6. (a) Monthly rainfall and mean temperature variations. (b) Time series of fluorescence intensity for travertine pools and soil waters and daily rainfall events. Some important rainfall events are represented by letters a–i. (c) Fluorescence intensity variations for rapid flow sites (FR and EIF). Dashed lines represent the mean values of FI, respectively, for the time intervals *X1* and *X2* (see Table 2).

during rainwater infiltration through soil and rock pores than to increases in DOC concentrations.

FI variations in fast dripping waters (EIF and FR, mean discharge of 818 and 3.5×10^5 ml/h, respectively), compared to rainfall events, are presented in Fig. 6c. The FI of fast drip waters exhibits good correlation with individual and weekly rainfall events because of the drip flow characteristics. Higher discharge and shorter residence time are apparently the causes of faster transport of the organic matter in the water feeding these stalactites.

The peaks of FI are correlated with more intense rain events occurring preferentially during periods of higher temperatures (Fig. 6a and c). On the other hand, during periods of decreased frequency and intensity of rainfall events or lower temperatures, FI exhibits little variation and values tend to define a baseline. This FI behavior is attributed to the lower efficiency in the transport of fluorescent organic substances during drier periods and to changes in humification rates in soil due to temperature variations (McGarry and Baker, 2000). In addition, water movement in fissured aquifers is also dependent upon hydraulic pressure, which increases with more intense rainfall events, as in a piston flow system (Genty and Deflandre, 1998). This affects water composition by pushing the SOM into the aquifer more rapidly, but the timing-to-peak will correspond to the particular hydrologic conditions at each site.

Relations between FI variations and changes in rainfall and temperature are demonstrated in Fig. 6a and c. For example, the lower values of FI in FR drip waters observed between September and November of 2000 are probably connected with lower temperatures in winter months (June–July of 2000) rather than rainfall events, because even under favored SOM transport conditions in the system, no significant FI variations were recorded, as can be seen in event *a* ($\Sigma = 216$ mm; 8/27/2000 to 9/17/2000 or days 27–48; Fig. 6c).

The FI values of FR waters started to increase simultaneously with higher temperatures and more effective rainfall events in summer (Fig. 6a). This is illustrated by combining events *b, c* and *d* (total amount = 344 mm, corresponding to 57 days) with great FI variations (Fig. 6c). Between February and April of 2001, FI in both FR and EIF curves was invariably low due to decreased rainfall. This tendency changed after August 2001 with remarkable increases in FI, in parallel with more isolated rainfall events (events *e, f, g* and *h*, Fig. 6c), together with the anomalously high mean monthly winter temperature of that year. The FI curves again showed great variability after the beginning of summer rainfall events in December 2001, marked by event *i* (Fig. 6c).

4.4.2. Discharge and FI variations in slow drip stalactites

In order to compare FI and discharge variations of slow drip waters, the ESF and EE2 stalactites were monitored during approximately 2 years using an automatic tipping-bucket gauge. The results are shown in Fig. 7b. EE1 discharges were obtained measuring the time to fill a recipient of known volume.

In the case of slow drip flow, the response to rainfall events is strongly controlled by overlying rock thickness which is 100 m at ESF and 300 m at both EE1 and EE2. Change in dripping relative to the onset of rainfall events is influenced by soil cover and limestone microfissure network, which in some cases means a time lag of several months before rain water recharge begin to affect drip discharge (Genty and Deflandre, 1998; Ayalon et al., 1998).

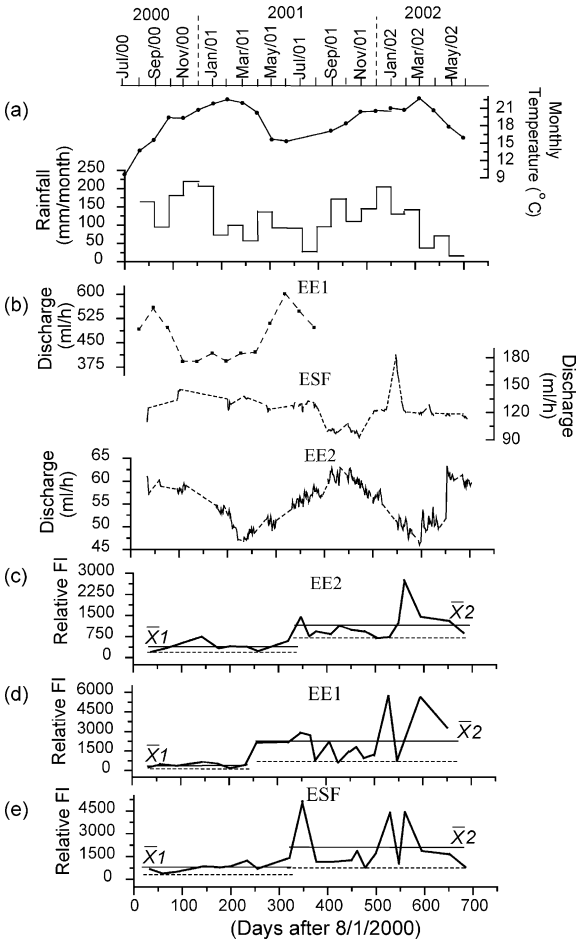

Fig. 7. (a) Monthly rainfall and mean temperature variations. (b) Drip discharge variation with time for slow drip waters at ESF Site, located at 100 m from surface and EE1 and EE2 sites, both located at 300 m from surface. Dashed lines mark periods without measurements. (c) Time series of fluorescence intensity for slow drip waters at ESF site. (d) EE1 site and (e) EE2 site. Solid and dashed lines represent the mean and lower values of FI, respectively, for the time intervals *X1* and *X2* (see Table 2).

Discharge of the ESF stalactite ranged from 92 to 182 ml/h (Table 1). Response time of drip discharge to changes in precipitation was estimated as 1 week to a month, based on comparisons with ESF discharge (Fig. 7b) and rainfall variations (Fig. 7a). EE1 stalactite discharges ranged between 390 and 600 ml/h yet showed no correspondence to monthly rainfall variations. Drip discharge for the EE2 stalactite (46–63 ml/h) describes a relatively smooth, regular curve over 2 years (Fig. 7b).

The EE2 discharge curve in Fig. 7b is asymmetric, characterized by a longer rising limb of 7 months and a shorter recession limb of 5 months. During the 2 years, maximum and minimum drip discharge occurred respectively in October and March, despite differences in timing of the rainiest months for this period (Fig. 7a). This suggests that rain water was gradually stored in the fissured aquifer and that discharge increased at the beginning of each rainy season as a result of increased hydraulic pressure. This observation is in agreement with stalactite flow studies undertaken in a Belgian cave by Genty and Deflandre (1998).

The mean values of FI at EE1, EE2 and ESF sampling sites (Table 1) are respectively 1699 ± 1587 ($n=22$), 856 ± 875 ($n=23$) and 1576 ± 1316 ($n=22$). Time series of FI for these drip waters showed similarities in trends, except for eventual small differences in peak positions. The main similarities are observed in FI values for ESF and EE1, whose means were not significantly different according to the Anova Test ($p=0.78$, $\alpha=0.05$, $n=20$). In contrast, differences between variations of FI at EE1 and EE2 sampled at the same depth in the cave were confirmed by the above statistical procedure ($p=0.02$, $\alpha=0.05$, $n=22$). For example, the FI curve for EE2 waters is smooth, with fewer peaks in comparison with the curves for ESF and EE1 waters which is attributed to relatively lower drip discharges and higher residence time for EE2. Although FI time series for slow drip waters exhibited similarities at sampling sites at

Table 2
Results from interannual fluorescence intensity variations for drip waters

Sampling site	Mean[a]	Interval I				Interval II			
		Sampling period	Mean	SD	Range	Sampling period	Mean	SD	Range
EE1	1699	09/02/00 to 03/20/01	411	163	470	03/20/01 to 06/15/02	2300	1598	5100
EE2	856	09/02/00 to 06/15/01	400	171	523	06/15/01 to 06/15/02	1149	521	2031
ESF	1576	09/02/00 to 06/15/01	827	321	1019	06/15/01 to 06/15/02	2094	1513	4331
EIF	2758	09/02/00 to 07/12/01	918	320	782	07/12/01 to 06/15/02	3929	3056	9990
FR	1166	09/02/00 to 07/27/01	603	536	1721	07/27/01 to 06/15/02	1637	1617	5883

[a] Refers to the total sampling period (09/02/00 to 06/15/02).

contrasting depths, no correlations could be made between FI and rainfall events or drip discharge.

Differences of FI ranges among slow drip waters are also associated with variations in discharge. The higher the drip discharge, the higher the range of FI for waters collected at the same depth in the cave, as for example at EE1 (FI range = 5562, discharge = 470 ml/h) as compared to EE2 (FI range = 2553, discharge = 55 ml/h). From these observations, it is here suggested that larger variability of fluorophore concentration in drip waters may be expected under both relatively faster flow conditions and thinner rock cover as a result of more intense water replacement throughout the year. For example, the ranges of FI at the relatively shallow ESF site (100 m) and the deeper EE1 site (300 m) differ by only 17% (4741 vs. 5562, respectively) despite the great differences in their mean discharges (53% higher at the deeper locality), indicating that higher discharge compensates for the effect of thicker rock cover in this case (120 vs. 470 ml/h, respectively).

4.4.3. Interannual variations

Figs. 6c and 7c–e show interannual variations of FI in the drip water curves At all sites FI shows two distinct behaviors, clearly demonstrated by their mean and minimum values, standard deviation and range, all of which are comparatively lower at the beginning of the monitoring (Interval I) and higher for the remainder of the period (Interval II). The duration of the Interval I, varied from site to site, as follows: from September 2000 to March 2001 for EE1 samples, September 2000 to June 2001 for EE2 and ESF samples, and September 2000 to July 2001 for FR and EIF samples (Table 2).

As is observed in Fig. 7c–e, the curves for FI in the slow drip waters are much smoother for the Interval I than for Interval II. For fast drip waters, a similar trend is also evident, especially at EIF (Fig. 6c).

Another significant interannual difference is the increase in the minimum values for FI in interval II. During both intervals, minimum and near-minimum values were measured on several occasions, defining distinct background levels for FI (dashed lines in Fig. 7c–e) for each interval. This variation in background levels of FI may be correlated to differences in winter temperatures in the two intervals. Although mean summer temperatures were quite similar in both intervals, the mean winter temperature was 5.5 °C higher in 2001 than in 2000. In this case, a variation in local climate (increased temperature and more isolated rainfall events) was directly related to a significant variation in FI. Drawing on the work of McGarry and Baker (2000), this may be explained as the effect of increased humification rate of organic matter in the soil during the hotter period on the substances responsible for luminescence properties of the water.

5. Conclusions

The monitoring of fluorescence intensity (FI) and dissolved organic carbon (DOC) in runoff, soil,

and cave percolation waters demonstrated significant time-series variations in both, although no important correlations were observed between them. In addition, remarkable FI variations were observed at all sampling sites despite the similarities in DOC concentrations, even for soil waters and drip waters from different depths. Annual maximum value for DOC systematically occur following the rainiest period of the year.

Values of FI cannot be directly related to DOC content in the vadose aquifer of Santana cave, rather FI variations are more probably related to the nature of the organic matter than to the concentration of dissolved organic carbon. Thus, the processes responsible for DOC variation are probably not the same as those that increase FI values in the system. Further research on the composition of SOM in the water is required to understand the physical-chemical and hydrological processes that controll the composition, transport and proportions of the subcomponents of SOM in solution over long distances in a karst aquifer.

Comparisons of FI variations in drip waters at depths of 100 and 300 m with discharges between 55 and 3.5×10^5 ml/h indicate that FI is inversely proportional to depth and directly proportional to discharge. However, the combined influence of these parameters makes it difficult to compare FI among drip waters. For example, for fast drips a correlation was observed between subannual variations of FI and increases in both rainfall and temperature. In contrast, this correlation is not observed for slow drip waters. Therefore, all drip waters showed relevant differences in their interannual FI behavior from September 2000 to May 2002, which were correlated to changes in climatic parameters, mainly an increase of 5.5 °C in the mean winter temperature for 2001.

Based on the high variability of the FI signal identified in the present study for cave drip waters, it can be suggested that the fluorescence peaks of calcite in speleothems deposited under same conditions such as those described here, may not represent an annual signal, even for those formed under higher drip discharge. On the other hand, the observed relationship between mean FI variation of dripwater and interannual changes in temperature and precipitation suggest the potential use of *mean* values, rather than peak values, of fluorescent intensity in speleothem calcite as a paleoclimate proxy.

Acknowledgements

We thank the Fundação de Amparo a Pesquisa do Estado de São Paulo (FAPESP) for financial support of this research (Grant 99/10351-6 to I. Karmann and scholarships to F.W. da Cruz Jr. and G.B. Magdaleno). We thank Jurandir Santos and PETAR State Park Staff for supporting field work, Thomas Fairchild and Ian McReath for text revision. We thank Sandra Andrade (IGc-USP) and Aluísio Soares (UFSCAR) for caring out samples to ICP-OES and DOC analysis, respectively.

References

Ayalon, A., Bar-Matthews, M., Sass, E., 1998. Rainfall recharge relationship within a Karstic terrain in the eastern Mediterranean semi-arid region, Israel. Journal of Hydrology 207, 18–31.

Baker, A., Barnes, W.L., 1998. Comparison of the luminescence properties of waters depositing flowstone and stalagmites at Lower Cave, Bristol. Hydrological Processes 12, 1447–1459.

Baker, A., Genty, D., 1999. Fluorescence wavelength and intensity variations of cave waters. Journal of Hydrology 217, 19–34.

Baker, A., Smart, P.L., Edwards, R.L., Richards, D.A., 1993. Annual growth banding in a cave stalagmite. Nature 364, 518–520.

Baker, A., Barnes, W.L., Smart, P.L., 1996. Speleothem luminescence intensity and the spectral characteristics: signal calibration and a record of palaeoenvironmental change. Chemical Geology 130, 65–76.

Baker, A., Barnes, W.L., Smart, P.L., 1997. Variations in the discharge and organic matter content of stalagmite drip waters in Lower Cave, Bristol. Hydrological Processes 11, 1541–1555.

Baker, A., Proctor, C.J., Barnes, W.L., 1999a. Variations in stalagmite luminescence laminae structure at Poole's Cavern, England. AD 1910–1996: calibration of a palaeoprecipitation proxy. The Holocene 9 (6), 683–688.

Baker, A., Caseldine, C.J., Gilmour, K.A., Charman, D., Proctor, C., Hawkesworth, C.J., Philips, N., 1999b. Stalagmite luminescence and peat humification records of palaeomoisture for the last 2500. Earth and Planetary Science Letters 165, 157–162.

Balesdent, J., Chenu, C., Balabane, M., 2000. Relationship of soil organic matter dynamics to physical protection and tillage. Soil and Tillage Research 53, 215–230.

Campanha, G.C., Sadowski, G.R., 1999. Tectonics of the southern portion of Ribeira Belt (Apiaí Domain). Precambian Research 98, 31–51.

Charman, D.J., Caseldine, C., Baker, A., Gearey, B., Hatton, J., Proctor, C., 2001. Paleohydrological records from peat profiles and speleothems in Sutherland, Northwest Scotland. Quaternary Research 55, 223–234.

Coble, P.G., 1996. Characterization of marine and terrestrial Dom in seawater using excitation–emission matrix spectroscopy. Marine Chemistry 51, 325–346.

Coble, P.G., Green, S.A., Blough, N.V., Gagosian, R.B., 1990. Characterization of dissolved organic matter in the Black Sea by fluorescence spectroscopy. Nature 348, 432–434.

De Souza Sierra, M.M., Donard, O.F.X., Lamotte, M., Belin, C., Ewald, M., 1994. Fluorescence spectroscopy of coastal and marine waters. Marine Chemistry 47, 127–144.

Genty, D., Deflandre, G., 1998. Drip flow variations under a stalactite of the Père Noël cave (Belgium). Evidence of seasonal variations and air pressure constraints. Journal of Hydrology 211, 208–232.

Golchin, A., Oades, J.M., Skjemstad, J.O., Clarke, P., 1994. Soil structure and carbon cycling. Australian Journal of Soil Research 32, 1043–1068.

Kalbitz, K., 2001. Properties of organic matter in soil solution in a German fen area as dependent on land use and depth. Geoderma 104, 203–214.

Kalbitz, K., Solinger, S., Park, J.H., Mchalzik, B., Matzner, E., 2000. Controls on the dynamics of dissolved organic matter in soils: a review. Soil Science 165, 277–304.

Krauskopf, K.B., 1979. Introduction to Geochemistry. McGraw-Hill, New York pp. 617.

Linn, D.M., Doran, J.W., 1984. Effect of water-filled pore space on carbon dioxide and nitrous oxide production in tilled and nontilled soils. Soil Science Society of American Journal 48, 1267–1272.

MacDonald, N.W., Zak, D.R., Pregitzer, K.S., 1995. Temperature effects on kinetics of microbial respiration and net nitrogen and sulfur mineralization. Soil Science Society of American Journal 59, 233–240.

McCarthy, J.F., Williams, T.M., Liang, L., Jardine, P.M., Jolley, L.W., Taylor, D.L., Palumbo, A.V., Cooper, L.W., 1993. Mobility of natural organic matter in a sandy aquifer. Envirormental Science and Technology 27, 667–676.

McGarry, S.F., Baker, A., 2000. Organic acid fluorescence: applications to speleothem paleoenvironmental reconstruction. Quaternary Science Reviews 19, 1087–1101.

Nimer, E., 1989. Climatologia do Brasil. IBGE, Rio de Janeiro pp. 421.

Puget, P., Chenu, C., Balesdent, J., 1995. Total and young organic carbon distributions in aggregates of silty cultivated soils. European Journal of Soil Science 46, 449–459.

Senesi, N., Miano, T.M., Provenzano, M.R., Brunett, G., 1991. Characterization, differentiation, and classification of humic substances by fluorescence spectroscopy. Soil Science 152, 259–271.

Sollins, P., Homann, P., Caldwell, B.A., 1996. Stabilization and destabilization of soil organic matter: mechanisms and controls. Geoderma 74, 65–105.

Viana Jr., O., 2002. Hidroquímica, hidrologia e geoquímica isotópica (O e H) da fácies de percolação vadosa autogênica, caverna Santana, Município de Iporanga, Estado de São Paulo. Dissertação de Mestrado. Instituto de Geociências da Universidade de São Paulo.

Zogg, G.P., Zak, D.R., Ringelberg, D.B., MacDonald, N.W., Pregitzer, K.S., White, D.C., 1997. Compositional and functional shifts in microbial communities due to soil warming. Soil Science Society of American Journal 61, 475–481.